FLUID FLOW ANALYSIS AND VERTICAL GRADIENT FREEZE CRYSTAL GROWTH IN A TRAVELLING MAGNETIC FIELD

R. Lantzsch[1], *I. Grants*[2,3], *V. Galindo*[2], *O. Pätzold*[1], *G. Gerbeth*[2], *M. Stelter*[1], *A. Cröll*[4]

[1] *Institut für NE-Metallurgie und Reinststoffe, TU Bergakademie Freiberg, Germany (ronny.lantzsch@inemet.tu-freiberg.de)*
[2] *Forschungszentrum Rossendorf, MHD Department, Germany*
[3] *Institute of Physics, University of Latvia, 32 Miera, LV-2169 Salaspils, Latvia (ivanov@sal.lv)*
[4] *Kristallographisches Institut, Universität Freiburg (Br.), Germany*

Introduction. In bulk crystal growth of semiconductors the concept of remote flow control by means of alternating magnetic fields has attracted considerable interest (see, e.g., [1]–[6]). In this way the melt flow can be tailored for growth under optimised conditions to improve the crystal properties and/or the growth yield. A promising option is to apply an axially travelling magnetic wave to the melt (Travelling Magnetic Field – TMF). It introduces a mainly axial Lorentz force which leads to meridional flow patterns. In recent numerical studies [3],[6] the TMF has been recognised to be a versatile and efficient tool to control the heat and mass transport in the melt. For the Vertical Bridgman/Vertical Gradient Freeze (VB/VGF) growth, the beneficial effect of an adequately adjusted, TMF induced flow was clearly demonstrated in [6] in terms of the reduction of thermal shear stress at the solid-liquid interface.

In this paper we present experimental and numerical results on the TMF driven convection in an isothermal model fluid as well as first VGF-TMF crystal growth experiments. The model investigations are focused on the transition from laminar to instationary flow conditions that should be avoided in crystal growth applications. The VGF experiments were performed growing Ga doped germanium single crystals under the influence of the travelling field in a newly developed VGF-TMF equipment.

1. Experiment. The travelling field is created by an axisymmetric, equally spaced set-up of six coils, each of which is fed with a 60° phase-shifted current. In a good approximation the amplitudes of the radial and axial field components behave as continuous waves as indicated in Fig. 1*a*. Induction and frequency of the field can be varied between 0–5 mT and 50–800 Hz, respectively.

Details of the model experiments are shown in Fig. 1*b*. They were carried out at about 20°C with the travelling field applied to an InGaSn melt in cylindrical, non-conducting containers of different diameters. Axial velocity profiles (Fig. 1*c*) were measured near the side wall of the container by means of the Ultrasonic Doppler Velocimetry (UDV) method [10]. The basic flow characterised by the Reynolds number was investigated as a function of the aspect ratio, the magnetic force number and the shielding factor. The latter describe the relative influence of Lorentz force density and skin effect, respectively, on the fluid. According to the notation in Fig. 1 the relevant parameters of the problem read as follows:

$$\mathrm{Re} = \frac{uR}{\nu}\,, \qquad \mathrm{AR} = \frac{H}{R}\,, \qquad \mathrm{F} = \frac{\pi\sigma\omega B_0^2 H R^4}{2\eta\nu\lambda} \qquad \mathrm{S} = \mu_0\sigma\omega R^2$$

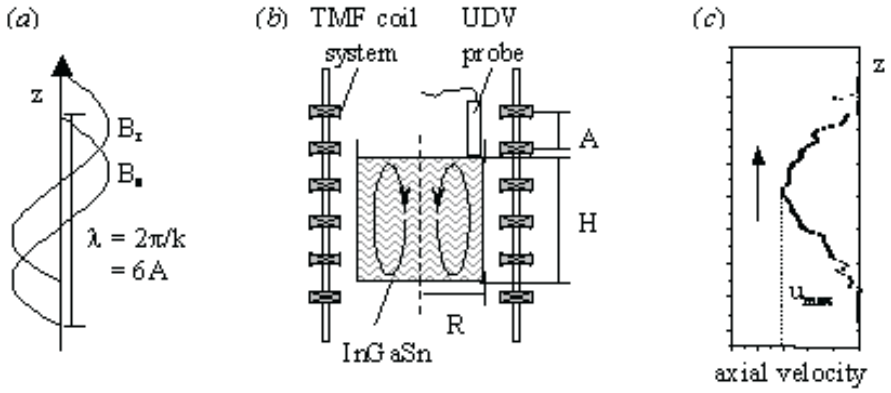

Fig. 1. (*a*) Radial and axial components of the TMF induction in a continuous wave model with $B_0 = (B_r^2 + B_z^2)^{1/2}$. (*b*) Schematic representation of the set-up used for the isothermal model experiments. The arrows indicate the flow pattern under the influence of an upward TMF. (*c*) Example of an axial velocity profile measured by the UDV probe near the container wall, with u_{max} as the maximum axial velocity being a characteristic value of the hydrodynamic system.

For the growth experiments a VGF furnace was equipped with the TMF coils (Fig. 2). The furnace was especially designed for the vapour pressure controlled VGF technique under optimised thermal conditions with the growth crucible arranged in a closed ampoule. It is characterised by a modular set-up of seven heating zones including a separate vapour pressure zone, a narrow seed zone, and an additional top heater in order to stabilize the temperature in the growth chamber. The maximum temperature of the furnace is about 1300°C and crystals with a diameter up to 3 in can be grown. The temperature control consists of a central computer system with implemented software controllers, DC power actuators for each heating zone, and a set of type B thermocouples, which are arranged at the inner surface of the ceramic heater supports.

Ga doped germanium single crystals with a diameter of 3 in were grown with the travelling field repeatedly switched on and off. The magnetic induction was deliberately chosen to give $F > F_c$ because the time-dependent flow is known to produce dopant striations due to microsegregation [4]. Hence, the impact of the TMF on the melt flow can be demonstrated by detecting such artificially induced striations. For this purpose the grown crystals were sliced longitudinally and the slices were etched in a $HNO_3 : HF : KMnO_4 : CH_3COOH$ solution to reveal the striation patterns.

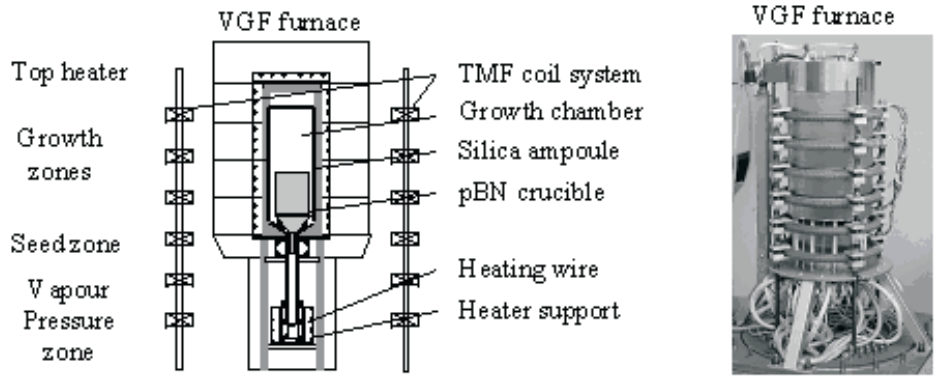

Fig. 2. Scheme (*a*) and photograph (*b*) of the VGF-TMF equipment used for the growth experiments.

2. Numerical simulation. The long wave condition of [7] was satisfied in our configuration since the inductor was much larger than the molten zone. The numerical linear instability study [7] was supplemented with results for the aspect ratio AR < 1. For this purpose the spectral simulation programs of [7] were used. First, the axisymmetric basic flow was found. The dynamics of separate azimuthally periodic perturbations with the wave number $m = 1, \ldots, 12$ were then considered by integrating numerically the linearised incompressible Navier–Stokes equations in time from random divergence free initial conditions. A few leading eigenvalues and eigenmodes were evaluated by the "snapshot method" [8]. The critical force number $\mathrm{F_c}$ was found as a root of a function describing the dependency of the real part of the leading eigenvalue on the force parameter. The critical Reynolds number was evaluated as a maximum of the axial velocity near the container wall at $\mathrm{F_c}$.

3. Results and discussion. Fig. 3 shows typical results of the InGaSn flow analysis. In Fig. 3*a* the Reynolds number based on the time-averaged value of the maximum axial flow velocity (see Fig. 1*c*) is plotted versus the magnetic force number for AR = 1. Under a weak travelling field an almost linear dependency is obtained. Beyond a certain critical TMF impact, however, the flow velocity rises non-linearly and more gradually with F. As illustrated by the insets in Fig. 3*a*, the transition to the non-linear behaviour is closely related to the appearance of time-dependent flow, which is at first periodic and later irregular at a higher force number. In Fig. 3*b* the critical Reynolds number indicating this transition is shown as a function of the aspect ratio.

The numerical results here are given in terms of the maximum axial velocity along the line of an UDV sensor averaged over the beam width. Deviations in Fig. 3*b* observed at a lower aspect ratio AR < 0.8 can be explained by the fact that the first instability is monotonic, characterised by the transition to an asymmetric stationary solution. The experiment, in turn, can only detect the secondary oscillatory instability. Besides, the deviations in Fig. 3 could be partially due to the shielding of the TMF, since the experimental data are taken from measurements with S = 3. The realistic field distribution and the resulting Lorentz force have been calculated by means of the commercial solver OPERA. For increasing field frequency this force distribution more and more differs from the simple analytical expression used in [7].

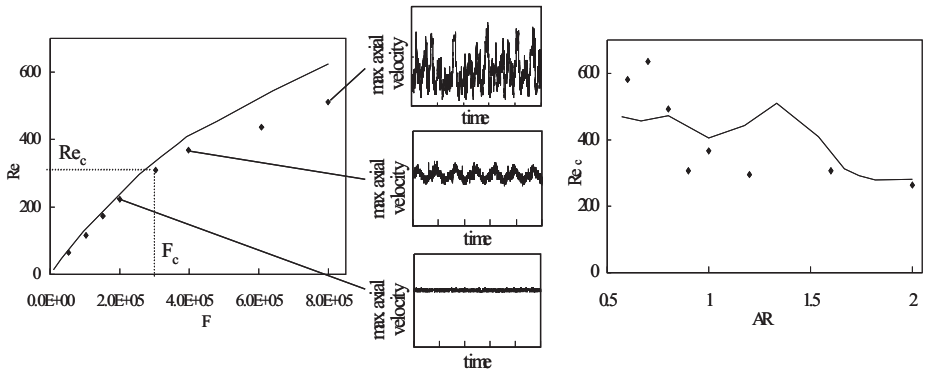

Fig. 3. Experimental (dots) and numerical (solid lines) results of the InGaSn flow analysis. (*a*) Re versus F plot for AR = 1 with the experimentally observed transition to a non-linear behaviour being indicated by the critical numbers $\mathrm{Re_c}$ and $\mathrm{F_c}$. For selected force numbers the corresponding UDV recordings are shown in detail to illustrate the transition from laminar to time-dependent flow. (*b*) Critical Reynolds number as a function of the aspect ratio.

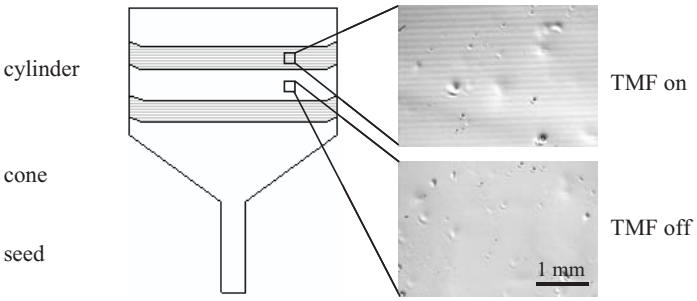

Fig. 4. Sketch of a longitudinal slice of a 3 in Ge:Ga single crystal grown under the influence of TMF pulses and microscopic images of selected surface sections showing a regular pattern of dopant striations due to a TMF-induced, time-dependent flow and a striation-free area grown without field.

Results of the VGF-TMF growth experiments are shown in Fig. 4. This crystal was grown under the influence of a downward travelling field which was switched on at melt aspect ratios of about 0.9 and 0.6 for two hours each. Frequency and induction of the field during the pulses were 50 Hz and 0.8 mT, respectively, giving S = 1 and F = 0.5–1.0×10^6. Obviously, a time-dependent melt flow is induced under these conditions as can be seen from regular striation patterns detected on the surface of a longitudinal crystal slice (Fig. 4). On the other hand, those parts of the crystal cylinder grown without field are essentially striation-free. These findings prove the capability of the developed equipment for the growth of VGF single crystals under the TMF influence. Growth experiments with optimised field parameters are under examination to confirm the effects predicted by numerical simulation [6].

Acknowledgements. The careful preparation of the experiments and the grown crystals by B. Geidel, K. Jenkner, and G. Uhlemann from the Institut für NE-Metallurgie und Reinststoffe is gratefully acknowledged. Financial support came from the Deutsche Forschungsgemeinschaft under contract CR 114/2-1. I.Grants was partially supported by European Commission under grant No. G1MA-CT-2002-04046.

REFERENCES

1. Y. M. Gelfgat, M. Abricka, J. Krumins. *Magnetohydrodynamics*, vol. 37 (2001), pp. 337–347.
2. V. Galindo, G. Gerbeth, W. v. Ammon, E. Tomzig, J. Virbulis. *Energy Conversation & Management*, vol. 43 (2002), pp. 309–316.
3. K. Mazuruk. *TAdv. Space Res.*, vol. 29 (2002), pp. 541–548.
4. O. Pätzold, I. Grants, U. Wunderwald, K. Jenkner, A. Cröll, G. Gerbeth. *J. Cryst. Growth*, vol. 245 (2002), pp. 237–246.
5. M. Bellmann, O. Pätzold, U. Wunderwald, A. Cröll. *Cryst. Res. Technol.*, vol. 39 (2004), pp. 193–197.
6. S. Yesilyurt, S. Motakef, R. Grugel, K. Mazuruk. *J. Cryst. Growth*, vol. 263 (2004), pp. 80–89.
7. I. Grants, G. Gerbeth. *J. Cryst. Growth*, vol. 269 (2004), pp. 630–638.
8. I. Goldhirsch, S. A. Orszag, B. K. Maulik. *J. Sci. Computing*, vol. 2 (1987), pp. 33–38.
9. M. Kurz, A. Pusztai, G. Müller. *J. Cryst. Growth*, vol. 198/199 (1999), pp. 101–106.
10. S. Eckert, G. Gerbeth, V. I. Melnikov. *Experiments in Fluids*, vol. 35 (2003), pp. 381–388.